Geomechanics and Engineering, *Vol. 42, No. 6 (2025) 441-452*
https://doi.org/10.12989/gae.2025.42.6.441

Experimental study on shrinkage characteristics of bentonite under different initial dry densities and water contents

Chunyuan Zhou[1a], Liang Kong[1,2b], Geng Niu*[1], Xiao Han[1c], Jiaqi Liu[2d] and Xinrui Wang[1e]

[1]*School of Science, Qingdao University of Technology, Qingdao 266520, China*
[2]*School of Civil Engineering, Qingdao University of Technology, Qingdao 266520, China*

(*Received June 15, 2025, Revised August 29, 2025, Accepted September 3, 2025*)

Abstract. Bentonite serves as a buffer/backfill material in deep geological repositories for high-level nuclear waste. From compaction to on-site installation, bentonite blocks undergo drying-induced shrinkage that can compromise the engineering barrier's mechanical integrity and radionuclide containment. In this paper, initially unsaturated bentonite is taken as the research object, and the indoor constant temperature drying test is carried out. The effects of initial dry density and initial water content on water evaporation, shrinkage deformation, and fracture evolution of bentonite are studied, respectively. The experimental results show that the initial dry density and initial water content have a significant effect on the water evaporation, shrinkage deformation, and crack evolution of bentonite. The larger the initial dry density or the smaller the initial water content, the less the water loss of bentonite in the evaporation process, the smaller the shrinkage deformation, and the fewer the number of cracks on the surface of bentonite. The shrinkage geometric factor can quantitatively describe the proportion of axial strain in the total volumetric strain. After drying, the shrinkage geometric factors of all compacted bentonite samples are between 1 and 3, which indicates that the axial strain accounts for a large proportion of the total volumetric strain, and the shrinkage deformation exhibits anisotropy. The effects of initial dry density and initial water content on water evaporation, shrinkage deformation, and fracture evolution of bentonite are closely related to their effects on inter-aggregate pores.

Keywords: bentonite; fracture evolution; initial dry density; initial water content; shrinkage deformation

1. Introduction

In recent years, with the rapid development of nuclear science, nuclear technology has not only been applied to the field of national defense, but also to agriculture, medicine, and people's production and life (Alzamel *et al.* 2022). However, with the rapid development, a large amount of high-level radioactive wastes (HLW) has been produced. High-level radioactive wastes have the characteristics of high radioactivity, high toxicity, long half-life, and large heat release. The migration of radionuclides to the external environment will cause serious harm to the biosphere. Therefore, the safe disposal of high-level radioactive waste is currently the most concerning environmental issue in all countries (Darda *et al.* 2021, Hoyer *et al.* 2021). Considering the disposal cost and disposal technology, deep geological disposal is considered to be the most feasible disposal scheme (Frankel *et al.* 2021, Kurgyis *et al.* 2024). Because of its low permeability, high expansibility, and strong nuclide adsorption capacity, bentonite is used as a good buffer/backfill material for deep geological disposal reservoirs to fill between waste tanks and stable rock masses to build a multi-scale barrier system (Kaufhold *et al.* 2019, Nazir *et al.* 2021, Ray *et al.* 2021, Villar *et al.* 2021). It is used to block the infiltration of groundwater, buffer the effect of surrounding rock pressure on waste tanks, and block the migration of nuclides to the external environment (Jalal *et al.* 2021, Kale *et al.* 2021, Shao *et al.* 2024, Song *et al.* 2024, Yoon *et al.* 2019).

Bentonite, as the main component of the buffer backfill material of the nuclear waste repository, its various design parameters that are still under research stage and there is no strict standard. The production of unsaturated bentonite blocks is usually pressed to the target dry density by professional equipment according to a certain water content in the factory. Due to the uncertainty of initial dry density and initial water content, there is no specific range of initial saturation. Bentonite needs to go through processes such as molding, handling, transportation, and operation. During this period, the bentonite block will experience drying, resulting in shrinkage deformation and even cracks, which will greatly damage the sealing integrity, mechanical stability, and nuclide blocking ability of the barrier system (Al-Mahbashi *et al.* 2023, Tan *et al.* 2024). Due to the influence of the surrounding environment, the saturation of bentonite blocks may range from 0-30% throughout the entire process.

*Corresponding author, Professor
E-mail: niugeng@qut.edu.cn
[a]Graduate student
[b]Professor
[c]Graduate student
[d]Graduate student
[e]Graduate student

ISSN: 2005-307X (Print), 2092-6219 (Online)

Previous research on soil shrinkage has identified four shrinkage phases: structural, normal, residual, and zero shrinkage (Braudeau *et al*. 1999) and has examined how initial dry density and water content influence compacted clays (Birle *et al.* 2008). At present, some research has also been carried out on the shrinkage deformation of bentonite. Tan *et al.* (2020) carried out a free drying test on a bentonite-sand mixture. It was found that for the compacted sample of bentonite-sand mixture, the compaction limited the permeability of the soil, resulting in a delay in evaporation and shrinkage deformation compared with the external soil. Considering the influence of initial water content, Zhang *et al*. (2022) carried out shrinkage and expansion tests on Heishan bentonite. The results showed that the shrinkage and expansion behavior of Heishan bentonite depended on the initial water content. Based on the vapor equilibrium method to control the suction, Song *et al*. (2024) carried out drying shrinkage tests on bentonite saturated with different concentrations of NaCl solution. Through the indoor drying test of the slurry bentonite-sand mixture, Zhang *et al*. (2019) found that only when the sand mixing rate is greater than 30%, the sand addition will significantly reduce the volume shrinkage of the sample. Wang *et al*. (2024) found that when the sand content in the bentonite-sand mixture exceeds 30%, these sands will form a sand skeleton, thereby limiting the further shrinkage of the bentonite-sand mixture. The above research on the shrinkage deformation of bentonite is more concerned with drying from saturation, and there are relatively few studies on drying from the initial unsaturated state. Secondly, the mechanism of the intrinsic relationship between bentonite shrinkage deformation, water evaporation, and fracture evolution is not clear.

Bentonite is a layered silicate mineral mainly composed of montmorillonite, which is very sensitive to water change. Therefore, the shrinkage deformation of bentonite blocks is often accompanied by cracks (Taheri and El-Zein 2023, Tan *et al*. 2024, Reijonen *et al*. 2020). Xu *et al*. (2022) expounded on the experimental research and application of fracture mechanics in soil cracking, and pointed out that it is necessary to combine soil mechanics and fracture mechanics to explain the theoretical model of soil cracking. Zhu *et al*. (2024) carried out a series of dry-wet cycle tests on expansive soil and combined with computer tomography and three-dimensional reconstruction technology to quantitatively study the cracking behavior of expansive soil. Tian *et al*. (2022) studied the effect of compaction state on the drying cracking behavior of cohesive soil. The results show that the compaction water content and dry density have an important influence on the development of cracks. At present, although a large number of experiments have been carried out on the dry shrinkage cracking of soil, there are few studies on the dry shrinkage cracking of bentonite. Secondly, the above research only focuses on the evolution process of cracks and pays less attention to shrinkage deformation. However, the evolution of cracks is closely related to the shrinkage deformation of soil.

In this paper, the compacted initial unsaturated bentonite is taken as the research object, and the indoor natural drying test is carried out. The effects of initial dry density and initial water content on the water evaporation, shrinkage characteristics, and fracture evolution of bentonite were studied, respectively. The influence mechanism of initial dry density and initial water content on the pore structure and shrinkage deformation of bentonite and the evolution law of fracture were analyzed. The relevant research results can provide a scientific basis for the safety design and construction of a high-level nuclear waste deep geological disposal repository.

2. Materials and methods

2.1 Materials and specimen preparation

The soil sample used in this test is Wyoming bentonite in the United States, which is sodium bentonite. The color of the soil sample is grayish white. The mineral composition of bentonite was analyzed by the XRD (X-ray Diffraction) technique, in which the content of montmorillonite was 77%, the content of quartz was 7%, the content of feldspar was 11%, and the content of gypsum was 5%. The external specific surface area was measured by N_2 adsorption. The total specific surface area was measured by the methylene blue method. The basic physical properties are shown in Table 1. The particle size distribution of bentonite was tested by a laser particle size analyzer, and the measurement results are shown in Fig. 1.

Considering that bentonite blocks absorb water and expand during service, their dry density will decrease, and an initial dry density of 1.2-1.5 g/cm^3 was selected for study. Moreover, the humidity in the tunnel is very high, and the blocks need to have a high initial water content to prevent them from absorbing moisture from the high-humidity environment of the disposal tunnel during installation, causing expansion and cracking of the blocks. Therefore, the initial water content (20%-35%) was adopted in this study. Air-dried bentonite was sieved (0.5 mm) and oven-dried at 105°C for 12 h, then cooled and stored in sealed bags. The soil sample with the target initial water content (20%-35%) was prepared by spraying a certain

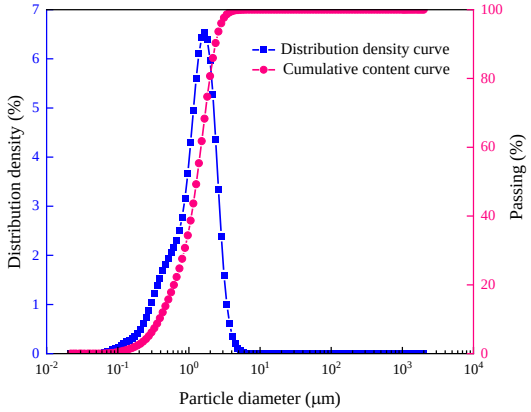

Fig. 1 Particle size distribution of bentonite

Table 1 Physical parameters of bentonite (Zhang *et al*. 2024)

Properties	Value	Exchangeable cations (meq/100 g)	Value
Specific Gravity (%)	2.70	Na^+	49.3
Liquid limit (%)	310.3	Ga^{2+}	31.2
Plastic limit (%)	28.8	Mg^{2+}	12.9
Total specific Surface area (m^2/g)	682.3	K^+	1.2
Total cation exchange capacity (meq/100 g)	72.9		

Table 2 The molding state variables in tests

specimen number	Initial dry density (g/cm^3)	Initial water content (%)	Pie-shaped specimen	
			Diameter (mm)	Height (mm)
D1.2	1.2	30	61.8	20
D1.3	1.3	30		
D1.4	1.4	30		
D1.5	1.5	30		
W20	1.4	20		
W25	1.4	25		
W30	1.4	30		
W35	1.4	35		

Note: D1.2 represents the sample with an initial dry density of 1.2, W20 represents the sample with an initial water content of 20%, and so on for the others

mass of distilled water into dry bentonite by the spray method. Put the prepared soil sample into a fresh-keeping bag and stand for more than 72 h. Then, a certain mass of wet soil is calculated using the initial dry density (1.2-1.5 g/cm^3) of the target and the initial water content of the target. The calculated wet soil was placed in a sample holder, and a hydraulic jack was used to prepare a ring cutter sample with a diameter of 61.8 mm and a height of 20 mm by static pressure. Compaction until there is no relative displacement between the upper and lower parts of the pressure sample mold, and keep the compaction state on the jack for 20 min. After that, the samples were directly removed from the mold and underwent a drying and shrinkage test.

2.2 Drying test and measurements

In this paper, eight groups of tests (Table 2) are designed to simulate the dry shrinkage deformation of bentonite from pressing to field construction. During the test, two parallel samples were prepared, respectively for D1.2-D1.5 and W20-W35, to test the repeatability of the test results. The diameter and height of the sample were measured with a vernier caliper (Accuracy of 0.01 mm) immediately after the demolding was completed. The mass was measured by an electronic balance (Accuracy of 0.01 g), and the sample was photographed by a camera. Then, the samples were placed in a constant temperature drying oven at a temperature of 20°C and a relative humidity of 43.2%, and the drying shrinkage test was carried out. One week before the test, the diameter, height, and mass of the sample were measured every 3 h, and photos of the sample were taken at the same time. One week later, the diameter, height, and mass of the sample were measured every 12 h, and photos of the sample were taken at the same time. When measuring the height and diameter of the sample, four measurement positions are selected and marked on average along the circumferential direction of the sample, and then the height and diameter of the four positions are measured and averaged during the test. When the mass of the sample changes by less than 0.01 g within 12 h, it is considered that the shrinkage process of the sample is completed. At this point, the test can be stopped. This test lasted for a total of 15 days. At the end of the test, it was found that the standard deviation of the measured data was about 0.031, and the coefficient of variation was about 0.152%. Secondly, the average value of the axial shrinkage deviation between the test sample and the parallel sample is 0.034, and the maximum value is 0.219. The average value of radial shrinkage deviation is 0.065, and the maximum value is 0.169. The average volume shrinkage deviation is 0.353, and the maximum value is 1.458. The error is very small, so this paper only analyzes the test samples.

These data can be used to calculate the water content and shrinkage deformation of bentonite during the drying process. The water content w, axial shrinkage strain ε_a , radial shrinkage strain ε_r, and volume shrinkage strain ε_v can be calculated according to formulas (1), (2), (3), and (4).

$$w = \frac{m - m_s}{m_s} \times 100\% \tag{1}$$

$$\varepsilon_a = \frac{h_0 - h}{h_0} \times 100\% \tag{2}$$

$$\varepsilon_r = \frac{d_0 - d}{d_0} \times 100\% \tag{3}$$

$$\varepsilon_v = \frac{v_0 - v}{v_0} \times 100\% \tag{4}$$

Where m represents the quality of the bentonite sample at a certain time. m_s represents the mass of the bentonite sample after drying. h_0, d_0, and v_0 respectively represent the height, diameter, and volume of the bentonite sample in the initial state. h, d, and v respectively represent the height, diameter, and volume of the bentonite sample at a certain time.

3. Experimental results

3.1 Moisture evaporation

Fig. 2(a) shows the variation of water content of compacted bentonite samples with time under different initial dry densities. The water content curves of the four groups of samples all presented a two-stage characteristic. In the initial stage, the water content decreased rapidly with the progress of evaporation, and then gradually tended to stabilize. The residual water content of samples D1.2, D1.3, D1.4, and D1.5 after evaporation is 8.45%, 8.16%, 7.85% and 7.25% respectively; that is, the larger the initial dry density, the smaller the residual water content. Furthermore,

it can be further found that for every 0.1 g/cm³ increase in the initial dry density, the residual water content decreases by approximately 0.4%, indicating that increasing the initial dry density can weaken the water-holding capacity of the soil in the stable stage. Fig. 2(b) further reveals the effect of initial water content on the evaporation effect of bentonite compaction samples. Although the variation trends of the water content curves of the four groups of samples are the same as those in Fig. 2(a), there are significant differences at the initial stage. The compacted bentonite samples with a higher initial water content have a higher water content at the same time point. However, the residual water content after reaching stability is basically the same. This indicates that the initial water content mainly controls the water gradient in the early stage of evaporation and has basically no influence on the final equilibrium state, which is consistent with the experimental results of Birle *et al.* (2008). In addition, W20, W25, W30, and W35 specimens evaporated 11.64%, 16.25%, 21.59%, and 26.84% of water throughout the drying period, respectively, which illustrates the fact that the greater the initial water content, the more water is evaporated.

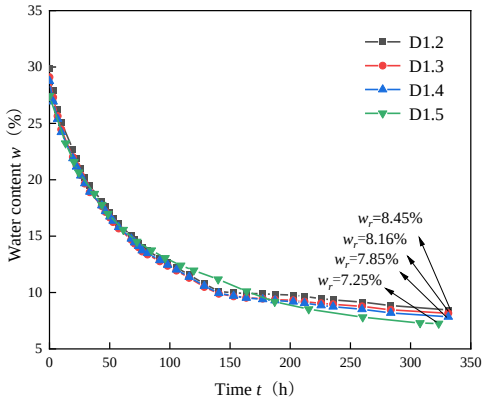

(a) Water content of bentonite samples with different initial dry density changes with time

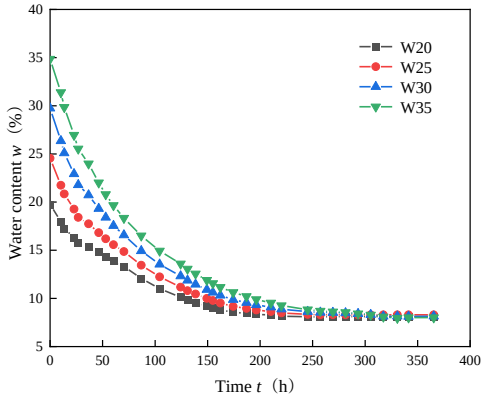

(b) The change of water content of bentonite samples wit different initial water content over time

Fig. 2 The change of water content of compacted bentonite samples with time in different initial states

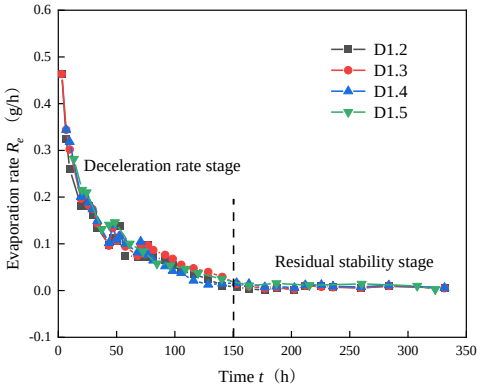

(a) The evaporation rate of bentonite samples with different initial dry density changes with time

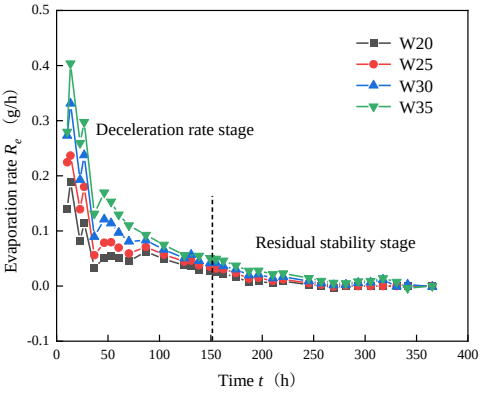

(b) The evaporation rate of bentonite samples with differer initial water content changes with time

Fig. 3 Variation of evaporation rate of compacted bentonite samples with different initial states with time

The evaporation rate is defined as the evaporation of water per unit time (g/h) (Tan *et al.* 2020). Fig. 3(a) is the relationship between the evaporation rate of bentonite samples with different initial dry densities and time. It can be seen from the figure that the overall change patterns of the evaporation rate curves of bentonite samples with different initial dry densities are basically the same. The evaporation rate decreases rapidly from 0 to 150 h and is in the deceleration stage. After 150 h, the evaporation rate gradually tended to stabilize and reached the residual stability stage. Although the initial dry density is different, the evaporation rate is basically the same in the whole evaporation stage, and in the residual stable stage, the evaporation rate of the four groups of samples is not more than 4%, which is close to zero. This phenomenon may be that although the enhanced compaction reduces the final water holding capacity of the soil, it also leads to the reorganization of the pore structure of the soil, increases the capillary resistance, and leads to the dynamic balance between the evaporation driving force and the resistance. In addition to the initial dry density, initial water content has a significant influence on the rate of evaporation. Fig. 3(b)

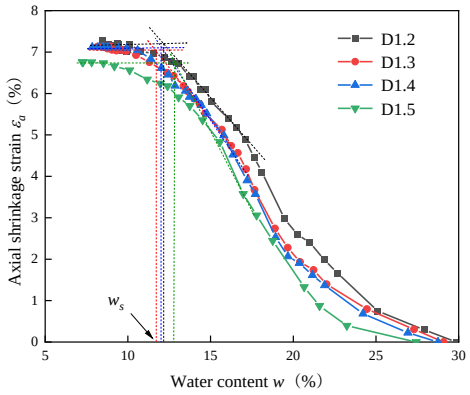

(a) Variation of axial shrinkage strain with water content

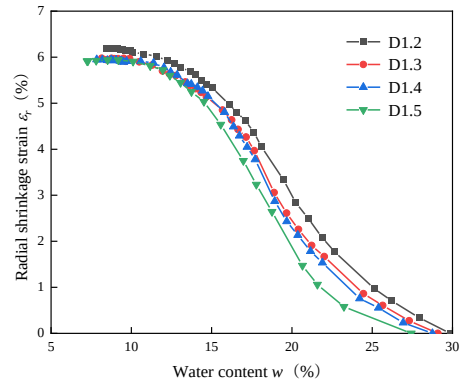

(b) Variation of radial shrinkage strain with water content

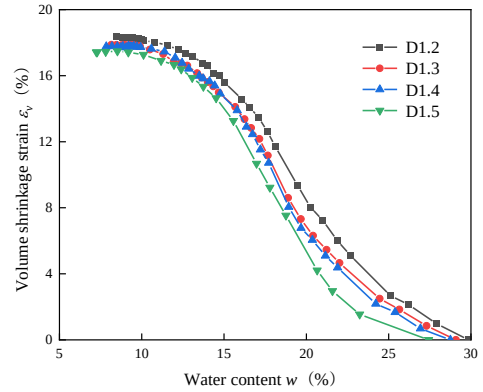

(c) The change of volume shrinkage strain with water content

Fig. 4 Shrinkage strain curves of compacted bentonite samples with different initial dry densities

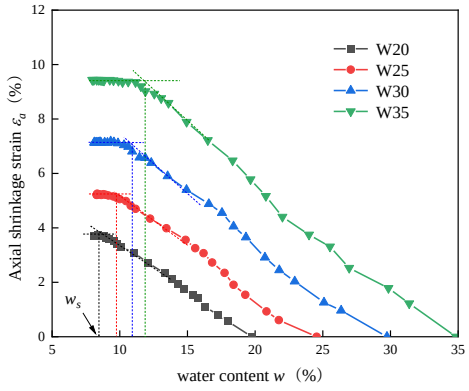

(a) Variation of axial shrinkage strain with water content

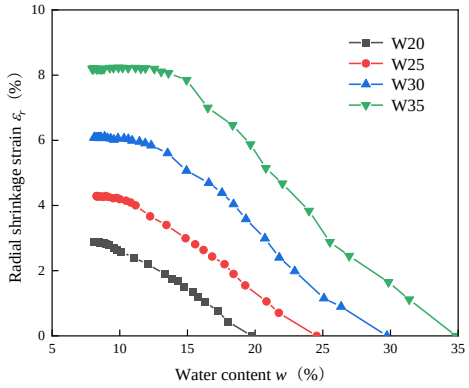

(b) Variation of radial shrinkage strain with water content

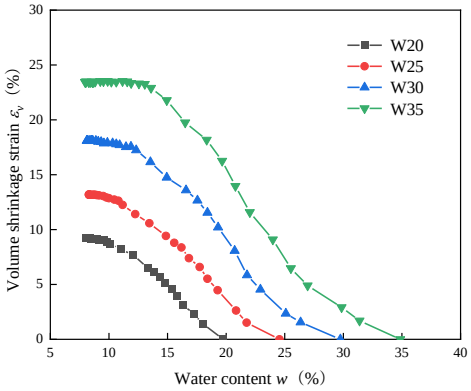

(c) The change of volume shrinkage strain with water content

Fig. 5 Shrinkage strain curves of compacted bentonite samples with different initial water contents

reveals the effect of initial water content on evaporation rate. In the deceleration rate stage (0~150 h), the higher the initial water content of the compacted bentonite sample, the higher the evaporation rate. The average evaporation rates of W20, W25, W30, and W35 samples were 0.059, 0.083, 0.110, and 0.141 g/h, respectively. However, when entering the residual stable stage (after 150 h), the evaporation rate is basically the same and tends to zero.

3.2 Shrinkage deformation

Figs. 4(a)-4(c) shows the relationship between shrinkage strain and water content of compacted bentonite samples with different initial dry densities. It can be seen from the figure that the overall variation trends of the shrinkage strain relationship curves of bentonite samples with different initial dry densities are basically the same. At the initial stage of drying, the axial

Fig. 6 Variation of fissures of compacted bentonite sample W35 with time

shrinkage strain, radial shrinkage strain, and volume shrinkage strain decreased rapidly with the decrease the axial shrinkage strain, radial shrinkage strain, and volume shrinkage strain finally tend to a stable value. Further analysis of the shrinkage test results in Figs. 4(a)-4(c) reveals that the final axial shrinkage strains corresponding to specimens D1.2, D1.3, D1.4, and D1.5 are 7.28%, 7.13%, 7.11%, and 6.76%, respectively. The corresponding final radial shrinkage strains were 6.19%, 5.98%, 5.95% and 5.91%, respectively. The corresponding final volume shrinkage strains were 18.36%, 17.87%, 17.77% and 17.42%, respectively. These test results show that the greater the initial dry density, the smaller the final axial shrinkage strain, final radial shrinkage strain, and final volume shrinkage strain of the compacted bentonite sample. In addition, when the initial dry density increases from 1.2 to 1.5, the final axial shrinkage strain decreases by 0.15%, 0.02% and 0.35%, respectively. The final radial shrinkage strain decreases by 0.21%, 0.03% and 0.04%, respectively. The final volume shrinkage strain decreases by 0.49%, 0.1% and 0.35%, . The above test results show that the change in initial dry density has a relatively small effect on the shrinkage and deformation of bentonite.

Figs. 5(a)-5(c) gives the relationship between the shrinkage strain of compacted bentonite samples with different initial water content and the change of water content. It can be seen from the figure that the final axial shrinkage strain, final radial shrinkage strain, and final volume shrinkage strain of sample W20 are 3.72%, 2.89% and 9.21% respectively. The final axial shrinkage strain, final radial shrinkage strain, and final volume shrinkage strain of sample W25 were 5.22%, 4.29% and 13.17% respectively. The final axial shrinkage strain, final radial shrinkage strain, and final volume shrinkage strain of specimen W30 are 7.14%, 6.08% and 18.09%, respectively.

The final axial shrinkage strain, final radial shrinkage strain, and final volume shrinkage strain of specimen W35 were 9.43%, 8.19% and 23.43%, respectively. By comparing these test results, it can be found that with the increase of initial water content, the final axial shrinkage strain, the final radial shrinkage strain, and the final volume shrinkage strain all increase. Further from the diagram, it can be found that in the process of increasing the initial water content from 20% to 35%, the final axial shrinkage strain increases by 1.5%, 1.92% and 2.29%, respectively. The final radial shrinkage strain increases by 1.4%, 1.79% and 2.11%. The increase of the final volume shrinkage strain is 3.96%, 4.92% and 5.34%. The effect of initial water content on the shrinkage and deformation of bentonite is more pronounced than that of initial dry density.

The shrinkage limit of soil is the water content of soil when it changes from semi-solid to solid. When the water content of the soil reaches the shrinkage limit (w_s), the shrinkage deformation of the soil will no longer change with the decrease of the water content. The method of determining the shrinkage limit is to extend the straight line between the linear change section and the stable stage in the curve of axial strain with water content, and the water content corresponding to the intersection point is the shrinkage limit. From Figs. 4(a) and 5(a), it can be seen that the corresponding w_s of D1.2, D1.3, D1.4 and D1.5 bentonite samples are 12.18%, 11.71%, 12.02% and 12.74%, respectively; the corresponding bentonite samples of W20, W25, W30 and W35 were 8.35%, 9.76%, 10.96% and 11.97%, respectively. This illustrates the fact that the greater the initial dry density or initial water content of the bentonite, the greater the shrinkage limit of the soil.

The volume shrinkage of soil includes two parts, namely axial shrinkage and radial shrinkage. However, the axial shrinkage deformation and radial shrinkage deformation of the soil during the drying process are not equal, that is, the

Fig. 7 The final state of compacted bentonite samples with different initial dry densities after drying

Fig. 8 The final state of compacted bentonite samples with different initial water content at the end of drying

Table 3 Shrinkage geometric factors of bentonite in different initial compaction states

Sample No.	D1.2	D1.3	D1.4	D1.5	W20	W25	W30	W35
r_s	2.68	2.66	2.65	2.74	2.55	2.63	2.69	2.70

shrinkage deformation is anisotropic. It can be seen from Figs. 4(a), 4(b) and 5(a), 5(b) that the final axial shrinkage strains of D1.2, D1.3, D1.4, D1.5 and W20, W25, W30, W35 are all greater than the final radial shrinkage strains. To quantitatively describe the contribution of axial shrinkage and radial shrinkage to the total volume shrinkage during the shrinkage deformation of bentonite, the shrinkage geometric factor, r_s (Chertkov *et al.* 2004, Cornelis *et al.* 2006, Mishra *et al.* 2020, Sharanya *et al.* 2021) is introduced in this paper, and the correlation expression is

$$\left(1-\frac{\Delta v}{v_0}\right)=\left(1-\frac{\Delta h}{h_0}\right)^{r_s} \tag{5}$$

Where h_0 and v_0 represent the height and volume of the bentonite sample in the initial state, respectively. Δh and Δv represent the variation of height and volume of bentonite samples from the initial state to a certain time, respectively. The range of is r_s $1 \le r_s < \infty$. When $r_s=1$, the specimen only undergoes axial shrinkage deformation. When $1<r_s<3$, both axial shrinkage deformation and radial shrinkage deformation occur, but the shrinkage deformation is mainly axial shrinkage. When $r_s=3$, the axial shrinkage deformation of the sample is equal to the radial shrinkage deformation.

When $r_s>3$, the shrinkage deformation is mainly radial shrinkage. It can be known from Table 3 that the shrinkage geometric factors of D1.2, D1.3, D1.4, D1.5, and W20, W25, W30, W35 are $1<r_s<3$, indicating that the bentonite has both axial shrinkage deformation and radial shrinkage deformation, but the shrinkage deformation is mainly axial shrinkage. In conclusion, during the drying process of bentonite samples, the axial shrinkage deformation is greater than the radial shrinkage deformation, and the shrinkage deformation is mainly axial shrinkage.

3.3 Fracture evolution

In this paper, the time corresponding to the significant change of the surface morphology of the crack is used as the critical point to describe the evolution process of the crack with time during the drying process (Fig. 6). It is worth noting that the fracture evolution process of all samples in this paper, including parallel samples, is similar and contains obvious four-stage characteristics, but the critical time points corresponding to the change of fracture surface are different. In order to describe the complete evolution process of the crack during the dehumidification process in detail, this paper only describes the W35 sample as an example. Between 0 and 22 h, cracks are generated from the edge and develop rapidly to the center of the soil. At the same time, a crack network is gradually formed on the surface of the soil. The cracks in this stage are called the main cracks, and this stage can be called the edge-to-center crack expansion period. Between 22 and 78 h, the fracture gradually closed from the center to the edge, and the fracture network gradually disappeared. At this stage, the fracture development reached the fracture closure period. Between 78 h and 150 h, the main fracture redeveloped, which can be called the secondary development period of the main fracture. After 150 h, the fracture development gradually stabilized, and the fracture development reached a stable period of fracture.

Fig. 7 shows the final state of compacted bentonite samples with different initial dry densities after drying. It can be seen from Fig. 7 that the larger the initial dry density, the fewer the number of cracks generated after the drying of the bentonite sample, but the larger the width of the main crack. In addition to the initial dry density, the initial water content also has a significant influence on the development of cracks in bentonite. It can be seen from Fig. 8 that with the increase of initial water content, the number of cracks increases significantly, and the length and width of cracks increase. When the initial water content was less than 20%, no visible cracks were found in the bentonite samples to the

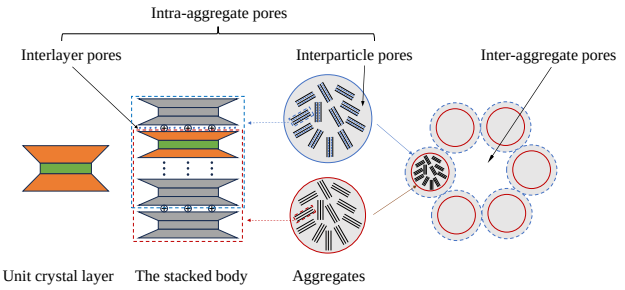

Fig. 9 Bentonite microstructure and microscopic pore structure (Modified from (Chen *et al*. 2021)

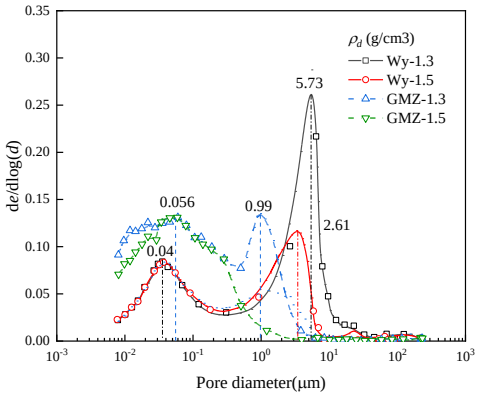

Fig. 10 Pore size distribution of bentonite with different initial dry density (Liang 2021)

naked eye. By comparing Figs. 7 and 8, it can be found that the influence of the initial water content on the final fracture morphology of the bentonite surface is significantly higher than that of the initial dry density.

4. Discussion

4.1 The influence of pore structure and initial state of bentonite on pore structure

At present, it is generally believed that the microscopic basic unit of bentonite is divided into a unit crystal layer, stacked body (Clay particles), and aggregates (Fig. 9) (Chen and Li 2024, Li *et al.* 2025). These three microstructures correspond to three pore types of bentonites, which are interlayer pores, interparticle pores, and inter-aggregate pores (Large pores). Among them, most scholars refer to the interlayer pores and the interparticle pores as the intra-aggregate pores (Small pores) (Dong *et al*. 2023). Therefore, it is considered that bentonite has a typical dual-pore structure. The initial state, compaction degree, and dehumidification process will affect the inter-aggregate pores of bentonite, which in turn affects the water-force characteristics of bentonite (Chen *et al.* 2021, Navarro *et al.* 2015, Niu *et al*. 2020).

The effect of initial dry density on the pore structure of bentonite mainly affects the inter-aggregate pores and has little effect on the intra-aggregate pores. A large number of experimental results (Fig. 10) show that when the initial dry density of bentonite increases, the number and size of small pores (intra-aggregate pores) in bentonite remain basically unchanged, while the number and size of large pores (inter-aggregate pores) decrease significantly (Chen *et al.* 2021, Liang 2021). This means that increasing the initial dry density will lead to the compression of the inter-aggregate pores. The initial water content also has a significant effect on the inter-aggregate pores of bentonite. This may be related to the water molecular layer adsorbed between the crystal layers and the hydration of the cations between the crystal layers (Fig. 9). Among them, the unit crystal layer will adsorb 1-4 layers of water molecules. Due to the effects of dissociation, adsorption, and isomorphous replacement, the surface of the crystal layer of the stack is usually negatively charged, which will attract the cations in the solution to balance. The cation hydrates under the action of water molecules, and the surface of the clay particles will combine with a layer of water film. Due to the presence of a water film, clay particles are in contact with each other through the binding water film. For unsaturated soil, with the increase of initial water content, more clay particles will be hydrated on the surface, and the thickness of the combined water film will also become thicker, resulting in an increase in the interparticle pores, which in turn leads to an increase in the inter-aggregate pores. Zhang *et al*. (2018) conducted mercury intrusion tests (MIP) on Gaomiaozi bentonite with different initial water contents (Fig. 11), and found that the larger the initial water content, the larger the pore size of the inter-aggregate pores of bentonite. This further proves the influence mechanism of initial water content on the pore structure of bentonite.

4.2 Evaporation and shrinkage process of bentonite

The pore water in the soil can be divided into capillary water and adsorbed water according to its occurrence state (Lu *et al*. 2022). Capillary water mainly exists in the inter-aggregate pores, while adsorbed water mainly exists in the intra-aggregate pores. Under the action of the humidity difference (evaporation potential) between the inside and outside of the soil, the water molecules in the soil continue to escape into the outside atmosphere, while the capillary action and adsorption hinder the migration of water molecules to the outside world (Zeng *et al*. 2022). In the early stage of evaporation, the capillary water in the inter-aggregate pores (Large pores) escapes preferentially. Due to the weak blocking ability of large pores to water migration, the evaporation rate changes rapidly in the early stage of evaporation. With the progress of evaporation, the pore water between aggregates continuously decreases, and the inter-aggregate pores contract, increasing the resistance when capillary water escapes from the inter-aggregate pores. Meanwhile, as the capillary water decreases, the capillary action gradually weakens, while the adsorption action gradually strengthens (Chen and Zhang 2024). Therefore, during this process, the water-holding capacity of the soil gradually increases, and water molecules are less likely to escape into the atmosphere. In addition, with the

decrease in water, the gas/liquid interface in the pores of the soil gradually migrates to the interior of the soil, resulting in the extension of the diffusion path of water molecules, so the evaporation rate of the soil gradually slows down. This stage is the deceleration rate stage. Until the pore water inter-aggregate is completely evaporated, the pore water intra-aggregate begins to escape. On the one hand, compared with large pores, water molecules in small pores are more closely connected to the pore walls, making it less likely for the water molecules to escape. On the other hand, the pore water in small pores is entirely adsorbed water, and adsorbed water is very difficult to evaporate. At this time, the evaporation rate curve enters the residual stable stage.

During the drying process of the soil, due to the evaporation of pore water, according to the capillary theory, the radius of curvature of the liquid surface between the soil particles will increase, and the matrix suction of the soil will increase, increasing the effective stress of the soil. Under the action of effective stress, the soil particles will be close to each other, which is manifested as volume shrinkage macroscopically. However, during the dehumidification process, the inter-aggregate pores will shrink, while the intra-aggregate pores are basically unchanged (Liu *et al.* 2023). Therefore, the change of bentonite volume is actually only related to the change of inter-aggregate pores. The larger the initial dry density is, the smaller the inter-aggregate pores are, and the intra-aggregate pores are basically unchanged, which leads to a decrease in soil particle spacing and the space for shrinkage deformation of the soil. The larger the initial water content, the larger the inter-aggregate pores, which leads to a larger spacing between the soil particles, and the larger the space for the shrinkage deformation of the soil. In addition, for unsaturated soils, due to the larger initial water content, the more clay particles hydrate, and the thicker the thickness of the combined water film, the resistance to rearrangement of soil particles is reduced, which leads to more shrinkage deformation.

4.3 The influence mechanism of initial dry density and initial water content on the final fracture

In the process of evaporation and water loss of soil, due to the decrease in water, the matrix suction will increase, and then the tensile stress on the surface of the soil caused by suction will increase. When the tensile stress is greater than the tensile strength of soil, cracks will occur (Al-Jeznawi *et al.* 2021, Zhang *et al*. 2017).

The evaporation of water in the soil is an important factor for the formation of soil fissures. The dry shrinkage cracking of soil is closely related to factors such as the thickness of the soil layer, environmental temperature, and humidity, and these factors affect the development of soil fractures by influencing the evaporation rate of the soil (Cordero *et al.* 2021, Tang *et al*. 2021, Zeng *et al.* 2022). During the evaporation process of soil, due to the non-uniformity of the evaporation rate on the surface layer of the soil and the fact that the evaporation rate on the surface layer is significantly greater than that inside the soil during the evaporation process, the forces acting on soil particles in all directions are different, resulting in an extremely uneven distribution of the stress field in the soil and providing sufficient conditions for the formation of fractures. When the evaporation rate of the soil is small, on the one hand, the force of water molecules on the soil particles is small, on the other hand, the water molecules in the soil pores have sufficient time to maintain stability, and the difference in the local evaporation rate of the soil is small (Zeng *et al*. 2022, Zeng *et al.* 2025). When the evaporation rate is fast, due to the violent movement of water molecules, the force on soil particles is large, which also increases the mobility of soil particles. Secondly, the larger evaporation rate will lead to a significant increase in the difference in local evaporation rate of soil, and the soil is more likely to produce cracks. As the initial dry density increases, the inter-aggregate pores decrease, and the evaporation rate of the soil decreases, thereby inhibiting the generation of cracks. The larger the initial water content is, the larger the inter-aggregate pores are, and the higher the evaporation rate of the soil is, thus promoting the development of cracks.

5. Conclusions

Through conducting indoor constant-temperature drying tests on compacted bentonite samples with different initial dry densities and initial water contents, the influence of the initial compaction state on the evaporation characteristics, shrinkage deformation, and fracture evolution of bentonite was studied, and the following conclusions were obtained:

(1) The initial dry density and initial water content affect the evaporation characteristics of bentonite. The initial dry density increases, the residual water content is smaller; the greater the initial water content, the faster the evaporation rate, which is attributed to the initial dry density and initial water content have a significant effect on the inter-aggregate pores. Therefore, the storage environment of bentonite should be strictly controlled in practical engineering to reduce the loss of water inter-aggregate.

(2) The larger the initial dry density, the smaller the final shrinkage strain of bentonite and the larger the shrinkage limit. The greater the initial water content, the greater the final shrinkage strain and shrinkage limit of bentonite. This is because the larger initial dry density and initial water content reduce the pore size of bentonite inter-aggregate pores, thereby reducing the shrinkage potential.

(3) During the whole drying process, the evolution of bentonite cracks showed obvious four-stage characteristics. The greater the initial dry density or the smaller the initial water content, the fewer the final number of cracks in bentonite. Compared with the initial dry density, the initial water content has a more significant effect on the crack. The initial dry density and initial water content affect the evaporation rate by affecting the pore structure of bentonite, which in turn affects the final fracture morphology. Therefore, it is suggested that the initial high density of compacted bentonite should be higher than 1.5 g/cm^3, and the initial water content should be lower than 20%.

At present, there are still some shortcomings in the research of this paper. Because the cracks generated under the initial unsaturated state of bentonite are small and dense, these cracks

cannot be completely extracted by digital image technology alone, so they can only be qualitatively analyzed for their evolution process. Subsequent work will use computed tomography (CT) to quantitatively study the evolution of fractures. Secondly, due to the influence of the groundwater environment and the frequent occurrence of extreme climate, the influence of salt solution and dry-wet cycle on the shrinkage deformation of bentonite can be studied in the future.

Acknowledgements

This work was supported by the National Natural Science Foundation of China (Grant 42307236) and the Natural Science Foundation of Shandong Province (Grants ZR2024ME170, ZR2023QE001).

References

Al-Jeznawi, D., Sanchez, M. and Al-Taie, A.J. (2021), "Using image analysis technique to study the effect of boundary and environment conditions on soil cracking mechanism", *Geotech. Geol. Eng*., **39**, 25-36. https://doi.org/10.1007/s10706-020-01376-5.

Al-Mahbashi, A.M., Dafalla, M. and Al-Shamrani, M. (2023), "Predicting soil-water characteristic curves of expansive soils relying on correlations", *Geomech. Eng*., **33**(6), 625-633. https://doi.org/10.12989/gae.2023.33.6.625.

Alzamel, M., Fall, M. and Haruna, S. (2022), "Swelling ability and behaviour of bentonite-based materials for deep repository engineered barrier systems: Influence of physical, chemical and thermal factors", *J. Rock Mech. Geotech*., **14**(3), 689-702. https://doi.org/10.1016/j.jrmge.2021.11.009.

Birle, E., Heyer, D. and Vogt, N. (2008), "Influence of the initial water content and dry density on the soil-water retention curve and the shrinkage behavior of a compacted clay", *Acta Geotech*., **3**, 191-200. https://doi.org/10.1007/s11440-008-0059-y.

Braudeau, E., Costantini, J.M., Bellier, G. and Colleuille, H. (1999), "New device and method for soil shrinkage curve measurement and characterization", *Soil Sci. Soc. Am. J*., **63**(3), 525-535. https://doi.org/10.2136/sssaj1999.03615995006300030015x.

Chen, Y.G., Cai, Y.Q., Pan, K., Ye, W.M. and Wang, Q. (2021), "Influence of dry density and water salinity on the swelling pressure and hydraulic conductivity of compacted GMZ01 bentonite-sand mixtures", *Acta Geotech*., 1-18. https://doi.org/10.1007/s11440-021-01305-7.

Chen, Y.G., Li, Z.Y., Ye, W.M. and Wang, Q. (2024), "Nanoscale mineral particle characteristics of Gaomiaozi bentonite", *Environ. Earth Sci*., **83**(19), 554. https://doi.org/10.1007/s12665-024-11865-y.

Chen, A., Zhang, X., Shi, X., Zhao, S. and Chen, J. (2024), "Study on the dry shrinkage characteristics and size effect of swell-shrink characteristic soil", *Plos one*, **19**(8), e0307679. https://doi.org/10.1371/journal.pone.0307679.

Chertkov, V.Y., Ravina, I. and Zadoenko, V. (2004), "An approach for estimating the shrinkage geometry factor at a moisture content", *Soil Sci. Soc. Am. J*., **68**(6), 1807-1817. https://doi.org/10.2136/sssaj2004.1807.

Cordero, J.A., Prat, P.C. and Ledesma, A. (2021), "Experimental analysis of desiccation cracks on a clayey silt from a large-scale test in natural conditions", *Eng. Geol*., 292, 106256. https://doi.org/10.1016/j.enggeo.2021.106256.

Cornelis, W.M., Corluy, J., Medina, H., Diaz, J., Hartmann, R., Van Meirvenne, M. and Ruiz, M.E. (2006), "Measuring and modelling the soil shrinkage characteristic curve", *Geoderma*, **137**(1-2), 179-191. https://doi.org/10.1016/j.geoderma.2006.08.022.

Darda, S.A., Gabbar, H.A., Damideh, V., Aboughaly, M. and Hassen, I. (2021), "A comprehensive review on radioactive waste cycle from generation to disposal", *J. Radioanal. Nucl. Ch*., **329**(1), 15-31. https://doi.org/10.1007/s10967-021-07815-8.

Dong, X.X., Chen, Y.G., Ye, W.M. and Wang, Q. (2023), "Modeling of water retention behavior of densely compacted Gaomiaozi bentonite based on pore structure evolution", *Eng. Geol*., **313**, 106977. https://doi.org/10.1016/j.enggeo.2022.106977.

Frankel, G.S., Vienna, J.D., Lian, J., Guo, X., Gin, S., Kim, S.H., Du, J., Ryan, J.V., Wang, J., Windl, W. and Taylor, C.D. (2021), "Recent advances in corrosion science applicable to disposal of high-level nuclear waste", *Chem. Rev*., **121**(20), 12327-12383. https://doi.org/10.1021/acs.chemrev.0c00990.

Hoyer, E.M., Luijendijk, E., Müller, P., Kreye, P., Panitz, F., Gawletta, D. and Rühaak, W. (2021), "Preliminary safety analyses in the high-level radioactive waste site selection procedure in Germany", *Adv. Geosci*., **56**, 67-75. https://doi.org/10.5194/adgeo-56-67-2021.

Jalal, F.E., Xu, Y., Li, X., Jamhiri, B. and Iqbal, M. (2021), "Fractal approach in expansive clay-based materials with special focus on compacted GMZ bentonite in nuclear waste disposal: A systematic review", *Environ. Sci. Pollut. R*, **28**, 43287-43314. https://doi.org/10.1007/s11356-021-14707-7.

Kale, R.C. and Ravi, K. (2021), "A review on the impact of thermal history on compacted bentonite in the context of nuclear waste management", *Environ. Technol. Innov*., **23**, 101728. https://doi.org/10.1016/j.eti.2021.101728.

Kaufhold, S., Dohrmann, R., Degtjarev, A., Koeniger, P. and Post, V. (2019), "Mg and silica release in short-term dissolution tests in bentonites", *Appl. Clay Sci*., **172**, 106-114. https://doi.org/10.1016/j.clay.2019.02.008.

Kurgyis, K., Achtziger-Zupančič, P., Bjorge, M., Boxberg, M.S., Broggi, M., Buchwald, J., Ernst, O.G., Flügge, J., Ganopolski, A., Graf, T. and Kortenbruck, P. (2024), "Uncertainties and robustness with regard to the safety of a repository for high-level radioactive waste: introduction of a research initiative", *Environ. Earth Sci*., **83**(2), 82. https://doi.org/10.1007/s12665-023-11346-8.

Li, K.P., Chen, Y.G., Ye, W.M. and Wang, Q. (2025), "Self-sealing behavior of annular technological voids between compacted bentonite blocks: insights from the macro-and micro-perspectives", *Acta Geotech*., 1-22. https://doi.org/10.1007/s11440-024-02514-6.

Liang, W.Y. (2021), "Thermo-chemo-mechanical characteristics and microstructure evolution of compacted bentonite", Ph.D. Dissertation, Guilin university of technology. (in Chinese)

Liu, Z.R., Ye, W.M., Zhu, J.C., Chen, Y.G. and Wang, Q. (2023), "Temperature and alkaline solution effects on the hydro-mechanical behaviours of GMZ bentonite pellet mixtures", *Acta Geotech*., **18**(11), 6097-6110. https://doi.org/10.1007/s11440-023-02044-7.

Lu, N., Luo, S. and Zhou, B. (2022), "Water adsorption–induced pore-water pressure in soil", *J. Geotech. Geoenviron*., **148**(6), 04022042. https://doi.org/10.1061/(ASCE)GT.1943-5606.0002814.

Mishra, P.N., Zhang, Y., Bhuyan, M.H. and Scheuermann, A. (2020), "Anisotropy in volume change behaviour of soils during shrinkage", *Acta Geotech*., **15**, 3399-3414. https://doi.org/10.1007/s11440-020-01015-6.

Navarro, V., Asensio, L., De la Morena, G., Pintado, X. and

Yustres, Á. (2015), "Differentiated intra-and inter-aggregate water content models of mx-80 bentonite", *Appl. Clay Sci*., **118**, 325-336. https://doi.org/10.1016/j.clay.2015.10.015.

Nazir, M., Kawamoto, K. and Sakaki, T. (2021), "Properties of granulated bentonite mixtures for radioactive waste disposal: A review", *Int. J. Geomate*, **20**(81), 132-145. https://geomatejournal.com/geomate/article/view/213.

Niu, G., Shao, L., Sun, D.A. and Guo, X. (2020), "A simplified directly determination of soil-water retention curve from pore size distribution", *Geomech. Eng*., **20**(5), 411-420. https://doi.org/10.12989/gae.2020.20.5.411.

Peter, E. (2018), "Investigation of alternatives to the buffer protection[R]", [S.l.]: Svensk Kärnbränslehantering AB.

Ray, S., Mishra, A.K. and Kalamdhad, A.S. (2021), "Influence of real and synthetic municipal solid waste leachates on consolidation and shear strength behaviour of bentonites", *Environ. Sci. Pollut. R*, **28**, 30975-30985. https://doi.org/10.1007/s11356-021-12863-4.

Reijonen, H.M., Kuva, J. and Heikkilä, P. (2020), "Benefits of applying X-ray computed tomography in bentonite based material research focussed on geological disposal of radioactive waste", *Environ. Sci. Pollut. R*, **27**, 38407-38421. https://doi.org/10.1007/s11356-020-08151-2.

Shao, J., Sun, D.A., Zhou, X. and Zeng, Z. (2024), "Thermal conductivity of MX80 powders-granules mixture and its prediction for high-level radioactive waste repository", *Int. Commun. Heat Mass*, **155**, 107543. https://doi.org/10.1016/j.icheatmasstransfer.2024.107543.

Sharanya, A.G., Mudavath, H. and Thyagaraj, T. (2021), "Review of methods for predicting soil volume change induced by shrinkage", *Innov. Infrastruct. So*, **6**, 1-16. https://doi.org/10.1007/s41062-021-00485-1.

Song, Z., Zhang, Z., Lu, Y. and Du, X. (2024), "Shrinkage behavior of compacted bentonite considering physicochemical effects", *Sci. Total Environ*., **906**, 167547. https://doi.org/10.1016/j.scitotenv.2023.167547.

Taheri, S. and El-Zein, A. (2023), "Desiccation cracking of polymer-bentonite mixtures: An experimental investigation", *Appl. Clay Sci*., **238**, 106945. https://doi.org/10.1016/j.clay.2023.106945.

Tan, Y., Zhang, H. and Wang, Y. (2020), "Evaporation and shrinkage processes of compacted bentonite-sand mixtures", *Soils Found*., **60**(2), 505-519. https://doi.org/10.1016/j.sandf.2020.03.008.

Jalal, F.E., Xu, Y., Li, X., Jamhiri, B. and Iqbal, M. (2021), "Fractal approach in expansive clay-based materials with special focus on compacted GMZ bentonite in nuclear waste disposal: A systematic review", *Environ. Sci. Pollut. R*, **28**, 43287-43314. https://doi.org/10.1007/s11356-021-14707-7.

Kale, R.C. and Ravi, K. (2021), "A review on the impact of thermal history on compacted bentonite in the context of nuclear waste management", *Environ. Technol. Innov*., **23**, 101728. https://doi.org/10.1016/j.eti.2021.101728.

Kaufhold, S., Dohrmann, R., Degtjarev, A., Koeniger, P. and Post, V. (2019), "Mg and silica release in short-term dissolution tests in bentonites", *Appl. Clay Sci*., **172**, 106-114. https://doi.org/10.1016/j.clay.2019.02.008.

Kurgyis, K., Achtziger-Zupančič, P., Bjorge, M., Boxberg, M.S., Broggi, M., Buchwald, J., Ernst, O.G., Flügge, J., Ganopolski, A., Graf, T. and Kortenbruck, P. (2024), "Uncertainties and robustness with regard to the safety of a repository for high-level radioactive waste: introduction of a research initiative", *Environ. Earth Sci*., **83**(2), 82. https://doi.org/10.1007/s12665-023-11346-8.

Li, K.P., Chen, Y.G., Ye, W.M. and Wang, Q. (2025), "Self-sealing behavior of annular technological voids between compacted bentonite blocks: insights from the macro-and micro-perspectives", *Acta Geotech.*, 1-22. https://doi.org/10.1007/s11440-024-02514-6.

Liang, W.Y. (2021), "Thermo-chemo-mechanical characteristics and microstructure evolution of compacted bentonite", Ph.D. Dissertation, Guilin university of technology. (in Chinese)

Liu, Z.R., Ye, W.M., Zhu, J.C., Chen, Y.G. and Wang, Q. (2023), "Temperature and alkaline solution effects on the hydro-mechanical behaviours of GMZ bentonite pellet mixtures", *Acta Geotech*., **18**(11), 6097-6110. https://doi.org/10.1007/s11440-023-02044-7.

Lu, N., Luo, S. and Zhou, B. (2022), "Water adsorption-induced pore-water pressure in soil", *J. Geotech. Geoenviron*., **148**(6), 04022042. https://doi.org/10.1061/(ASCE)GT.1943-5606.0002814.

Mishra, P.N., Zhang, Y., Bhuyan, M.H. and Scheuermann, A. (2020), "Anisotropy in volume change behaviour of soils during shrinkage", *Acta Geotech*., **15**, 3399-3414. https://doi.org/10.1007/s11440-020-01015-6.

Navarro, V., Asensio, L., De la Morena, G., Pintado, X. and Yustres, Á. (2015), "Differentiated intra-and inter-aggregate water content models of mx-80 bentonite", *Appl. Clay Sci*., **118**, 325-336. https://doi.org/10.1016/j.clay.2015.10.015.

Nazir, M., Kawamoto, K. and Sakaki, T. (2021), "Properties of granulated bentonite mixtures for radioactive waste disposal: A review", *Int. J. Geomate*, **20**(81), 132-145. https://geomatejournal.com/geomate/article/view/213.

Niu, G., Shao, L., Sun, D.A. and Guo, X. (2020), "A simplified directly determination of soil-water retention curve from pore size distribution", *Geomech. Eng*., **20**(5), 411-420. https://doi.org/10.12989/gae.2020.20.5.411.

Peter, E. (2018), "Investigation of alternatives to the buffer protection[R]", [S.l.]: Svensk Kärnbränslehantering AB.

Ray, S., Mishra, A.K. and Kalamdhad, A.S. (2021), "Influence of real and synthetic municipal solid waste leachates on consolidation and shear strength behaviour of bentonites", *Environ. Sci. Pollut. R*, **28**, 30975-30985. https://doi.org/10.1007/s11356-021-12863-4.

Reijonen, H.M., Kuva, J. and Heikkilä, P. (2020), "Benefits of applying X-ray computed tomography in bentonite based material research focussed on geological disposal of radioactive waste", *Environ. Sci. Pollut. R*, **27**, 38407-38421. https://doi.org/10.1007/s11356-020-08151-2.

Shao, J., Sun, D.A., Zhou, X. and Zeng, Z. (2024), "Thermal conductivity of MX80 powders-granules mixture and its prediction for high-level radioactive waste repository", *Int. Commun. Heat Mass*, **155**, 107543. https://doi.org/10.1016/j.icheatmasstransfer.2024.107543.

Sharanya, A.G., Mudavath, H. and Thyagaraj, T. (2021), "Review of methods for predicting soil volume change induced by shrinkage", *Innov. Infrastruct. So*., **6**, 1-16. https://doi.org/10.1007/s41062-021-00485-1.

Song, Z., Zhang, Z., Lu, Y. and Du, X. (2024), "Shrinkage behavior of compacted bentonite considering physicochemical effects", *Sci. Total Environ*., **906**, 167547. https://doi.org/10.1016/j.scitotenv.2023.167547.

Taheri, S. and El-Zein, A. (2023), "Desiccation cracking of polymer-bentonite mixtures: An experimental investigation", *Appl. Clay Sci*., **238**, 106945. https://doi.org/10.1016/j.clay.2023.106945.

Tan, Y., Zhang, H. and Wang, Y. (2020), "Evaporation and shrinkage processes of compacted bentonite-sand mixtures", *Soils Found*., **60**(2), 505-519. https://doi.org/10.1016/j.sandf.2020.03.008.

Tan, Y., Zhou, G., Zhang, H., Li, X. and Liu, P. (2024), "Effect of drying cracks on swelling and self-healing of bentonite-sand blocks used as engineered barriers for radioactive waste disposal", *J. Rock Mech. Geotech*., **16**(5), 1776-1787.

https://doi.org/10.1016/j.jrmge.2023.07.025.
Tang, C.S., Zhu, C., Cheng, Q., Zeng, H., Xu, J.J., Tian, B.G. and Shi, B. (2021), "Desiccation cracking of soils: A review of investigation approaches, underlying mechanisms, and influencing factors", *Earth-Sci. Rev.*, **216**, 103586. https://doi.org/10.1016/j.earscirev.2021.103586.
Tian, B.G., Cheng, Q., Tang, C.S., Zeng, H., Xu, J.J. and Shi, B. (2022), "Effects of compaction state on desiccation cracking behaviour of a clayey soil subjected to wetting-drying cycles", *Eng. Geol.*, **302**, 106650. https://doi.org/10.1016/j.enggeo.2022.106650.
Villar, M.V., Carbonell, B., Martín, P.L. and Gutiérrez-Álvarez, C. (2021), "The role of interfaces in the bentonite barrier of a nuclear waste repository on gas transport", *Eng. Geol.*, **286**, 106087. https://doi.org/10.1016/j.enggeo.2021.106087.
Wang, D.W., Zhu, C., Tang, C.S., Cheng, Q., Li, S.J. and Shi, B. (2024), "Experimental study on shrinkage characteristics of compacted bentonite-sand mixtures", *B Eng. Geol. Environ.*, **83**(1), 43. https://doi.org/10.1007/s10064-023-03521-9.
Xu, J.J., Tang, C.S., Cheng, Q., Xu, Q.L., Inyang, H.I., Lin, Z.Y. and Shi, B. (2022), "Investigation on desiccation cracking behavior of clayey soils with a perspective of fracture mechanics: a review", *J. Soil Sediment.*, 1-30. https://doi.org/10.1007/s11368-021-03082-y.
Yoon, S., Jeon, J.S., Kim, G.Y., Seong, J.H. and Baik, M.H. (2019), "Specific heat capacity model for compacted bentonite buffer materials", *Ann. Nucl. Energy*, **125**, 18-25. https://doi.org/10.1016/j.anucene.2018.10.045.
Zeng, H., Tang, C.S., Zhu, C., Vahedifard, F., Cheng, Q. and Shi, B. (2022), "Desiccation cracking of soil subjected to different environmental relative humidity conditions", *Eng. Geol.*, **297**, 106536. https://doi.org/10.1016/j.enggeo.2022.106536.
Zeng, H., Tang, C.S., Cui, Y.J. and Najdi, A. (2025), "Compressive stress induced by desiccation shrinkage in clayey soils", *Appl. Clay Sci.*, **267**, 107729. https://doi.org/10.1016/j.clay.2025.107729.
Zhang, H.Y., Tan, Y., Zhu, F., He, D.J. and Zhu, J.H. (2019), "Shrinkage property of bentonite-sand mixtures as influenced by sand content and water salinity", *Constr. Build Mater.*, **224**, 78-88. https://doi.org/10.1016/j.conbuildmat.2019.07.051.
Zhang, L. (2018), "Chemical and mechanical behaviour of GMZ bentonite and its predictions", Ph.D. Dissertation, Shanghai University. (in Chinese)
Zhang, X.D., Chen, Y.G., Ye, W.M., Cui, Y.J., Deng, Y.F. and Chen, B. (2017), "Effect of salt concentration on desiccation cracking behavior of GMZ bentonite", *Environ. Earth Sci.*, **76**, 1-10. https://doi.org/10.1007/s12665-017-6872-6.
Zhang, S.C., Li, K., Sun, K.M. and Wang, S. (2022), "Impact of initial moisture content on the shrinkage-swelling behavior of Heishan bentonite", *KSCE J. Civ. Eng.*, **26**(2), 550-555. https://doi.org/10.1007/s12205-021-0060-7.
Zhang, Q., Zhao, Y., Qin, L., Liang, W., Chen, K., Li, K. and Yan, R. (2024), "Adsorption properties of cesium by natural Na-bentonite and Ca-bentonite", *J. Radioanal. Nucl. Ch.*, **333**(11), 5347-5361. https://doi.org/10.1007/s10967-024-09627-y.
Zhu, X., Chen, Z., Ni, P., Cai, Z.Y., Huang, Y.H. and Zhang, C. (2024), "Cracking in compacted expansive soils under unidirectional wet-dry cycles: insights from X-ray computed tomography", *Acta Geotech.*, 1-14. https://doi.org/10.1007/s11440-024-02394-w.